Ocean Sci. Discuss., 10, 2207–2254, 2013
www.ocean-sci-discuss.net/10/2207/2013/
doi:10.5194/osd-10-2207-2013

Ocean Science
Discussions
Open Access

Spring-time zooplankton size structure over the continental shelf of the Bay of Biscay

P. Vandromme[1,6], E. Nogueira[2], M. Huret[3], Á. Lopez-Urrutia[2], G. González-Nuevo González[4], M. Sourisseau[1], and P. Petitgas[5]

[1]IFREMER, Centre Bretagne, Département Dynamique de l'Environnement Côtier, B.P. 70, 29280, Plouzané, France
[2]Centro Oceanográfico de Gijón, Instituto Español de Oceanografía, Gijón 33212, Spain
[3]IFREMER, Centre Bretagne, Laboratoire de Biologie Halieutique, B.P. 70, 29280, Plouzané, France
[4]Centro Oceanográfico de Vigo, Instituto Español de Oceanografía, Vigo 36200, Spain
[5]IFREMER, Centre Nantes, Département Écologie et Modèles pour l'Halieutique, rue de l'Île d'Yeu, 44300 Nantes, France
[6]GEOMAR, Helmholtz-Center for Ocean Science, Düsternbrooker Weg 20, 24105 Kiel, Germany

Received: 12 November 2013 – Accepted: 17 November 2013

– Published: 29 November 2013

Correspondence to: P. Vandromme (pvandromme@geomar.de) and M. Huret (mhuret@ifremer.fr)

Published by Copernicus Publications on behalf of the European Geosciences Union.

OSD
10, 2207–2254, 2013

Abstract

Linking lower ~~to~~ higher trophic levels requires a special focus on the pivotal role played by mid-trophic levels, i.e. the zooplankton. One of the most relevant information ~~on~~ zooplankton in term of fluxes of matter lies in its size structure. ~~We present here~~ an extensive dataset of size measurements covering part of the western European shelf and slope, from the Galician coast to the Ushant front, during springs from 2005 to 2012. Zooplankton size spectra were estimated using both measurements carried out in situ by the Laser-Optical Plankton Counter (LOPC~~, 816 records~~) and WP2 net (200 µm mesh size) samples ~~scanned~~ following the ZooScan methodology ~~and image analysis (a total of 89 samples were analyzed)~~. The LOPC counts and sizes all particles in the range 100 to 2000 µm of spherical equivalent diameter (ESD), whereas the WP2/ZooScan allows the counting, sizing and identification of zooplankton from ~ 400 µm ESD. The difference between the LOPC (all particles) and the WP2/ZooScan (zooplankton only) is assumed to provide the size distribution of non-living particles whose descriptors are further related to a set of explanatory variables (including physical, biological and geographic descriptors). A statistical correction based on these explanatory variables is then applied to LOPC measurements to remove~~d~~ the part due to non-living particles and estimate zooplankton size spectra. This extensive data set provides ~~a~~ new ~~look at regional and inter-annual variability of~~ the pelagic ecosystem of the Bay of Biscay.

1 Introduction

Size ~~matters and~~ pelagic~~s~~ ecosystems ~~are not an exception~~ (Stemmann and Boss, 2012). Physiological rates as well as predator~~-~~prey interactions of zooplankton are thought to be size-dependent (Peters and Wassenberg, 1983; Glazier, 2005; Barnes et al., 2011). Therefore, the zooplankton size structure ~~was~~ used as a powerful ecological indicator of the dynamics of zooplankton communities (Sheldon et al., 1972;

OSD
10, 2207–2254, 2013

Krupica et al., 2012) and is nowadays considered and resolved in an increasing number of ecosystem models (e.g., Baird and Suthers, 2007; Ward et al., 2012). In particular, size-based approach reveals appropriate in trophodynamics observation or modeling studies linking lower and upper trophic level ~~models~~ (Daewel et al., 2013), i.e. looking at potential top-down control on zooplankton, or estimating food availability to fish. For the latter case indeed, size of prey field is key, especially for fish larvae (e.g., anchovy and sardine, Poulet et al., 1996; Morote et al., 2010). To improve model realism, Daewel et al. (2008) first proposed a simple approach by sorting modeled zooplankton biomass in size classes according to the average slope of observed ~~in situ~~ zooplankton size-spectra. Size structured observations of the zooplankton are thus needed to provide prey field to fish models, investigate possible simplification through~~,~~ e.g., biomass ~~:~~ slopes relationships and to calibrate size structured zooplankton models.

However, measuring the size distribution of the zooplankton is not straightforward; various instruments exist, each of them having pros and cons. The size structure of the zooplankton could be measured by ~~in situ~~ particle~~s~~ counters such as the (Laser) Optical Plankton Counter (OPC and LOPC Herman et al., 2004) that measure the size of all particles crossing a light or laser field~~. The LOPC being able to count particles~~ from a diameter of 100 µm to few millimeters. ~~The~~ discrimination between living and non-living particles with these instruments is ~~however~~ not possible although using derived parameters, such as transparency, allows some discrimination for larger particles (> 2 mm for the LOPC) in particular cases (Checkley Jr et al., 2008). Recently, Petrik et al. (2013) proposed a way of discriminating small (< 2 mm) living and non-living particles counted by the LOPC by fitting a log-normal curve to the volume spectrum; residuals are considered to be living particles. Another way of measuring the zooplankton size structure is through traditional net samples followed by manual or automated counting and sizing (Vandromme et al., 2012). Even though this procedure may be the most accurate, the large amount of time required generally prevent its widespread use. The last way of measuring zooplankton size-structure is through in situ imaging systems (e.g., Picheral et al., 2010). ~~Yet~~, these instruments are still recent and not yet widely used to observe

OSD
10, 2207–2254, 2013

the zooplankton. In the present work, a combination of the LOPC (Herman et al., 2004) and net sampling followed by in-lab scanning of the samples (Vandromme et al., 2012) is used.

Few studies provide zooplankton biomass or size structure at the scale of the whole Bay of Biscay. Information is available either dispersed in time and space as reviewed by Poulet et al. (1996), as long time-series from transects but locally for the north of Spain (Valdés et al., 2007) or in front of the Gironde estuary (Albaina and Irigoien, 2004), from a single season and one (Nogueira et al., 2004) or two years (Sourisseau and Carlotti, 2006) as biomass and size structure of the mesozooplankton from an Optical Plankton Counter, or as a time-series of biomass and size-spectrum maps over the southern french shelf of the Bay over a decade in spring (Irigoien et al., 2009).

The objective of the present work is to propose an homogeneous estimation of the size structure of the zooplankton over the whole shelf of the Bay of Biscay, using an extensive dataset covering the period 2005–2012 in spring and a region running from the north of Portugal to Brittany in France. This by combining the use of an in situ Laser Optical Plankton Counter (LOPC, Herman et al., 2004) and from net samples (WP2 net) followed by an image analysis procedure (Zooscan (WP2/Zs) Gorsky et al., 2010; Vandromme et al., 2012). These two instruments allows the quantitative measurement of particles between 100 and ~2000 µm ESD (Equivalent Spherical Diameter) for the LOPC and between 400 and ~2500 µm ESD for the WP2 net (Nichols and Thompson, 1991; Vandromme et al., 2012) adapted to the sampling of the meso-zooplankton. Comparison between size structure observed by in situ particles counters and net catches generally show lower or equal estimates of abundance in each size by net catches (González-Quirós and Checkley, 2006; Schultes and Lopes, 2009; Gaardsted et al., 2010). This was attributed mainly to aggregates and detritus that are often not analyzed in net catches but also disaggregated by the net passage and thus not correctly sampled. E.g., González-Quirós and Checkley (2006) found that the abundance of particles estimated with the OPC in the size range of 1.26 to 6.35 mm ESD was 4 times higher than the abundance of zooplankton estimated by concomitant bongo net

OSD
10, 2207–2254, 2013

in the California current ecosystem. This is confirmed by in situ data from imaging systems were zooplankton accounts for a small portion of total particles (often less than 5 %, Stemmann and Boss, 2012). In the Bay of Biscay, Poulet et al. (1996) estimated the mesozoplankton biomass to be in the range of 4 to 20 % of the total Particulate Organic Carbon from a literature review. Fragile gelatinous zooplankton could also be destroyed by the net passage and therefore may account for part of the difference between in situ particles counters and net catches.

By investigating differences between size-spectra measured by the LOPC (zooplankton and non-living particles) and by the WP2/Zs (zooplankton only) we propose a statistical correction based on correlations between the differences observed and environmental data to estimate the zooplankton size-spectra where WP2/Zs data are missing. This allows the large available dataset from surveys made with the LOPC to be used for the characterization of the size structure patterns of the zooplankton in the Bay of Biscay. Estimated zooplankton size spectra are further investigated to depict correlations between total zooplankton biomass and the shape of the size distribution. We then discuss the results in terms of spatial and interannual variability of the habitats as defined by the size spectra distribution, as well as in terms of trophic transfer to upper trophic levels, in both an ecology and for a modelling perspectives.

2 Materials and methods

2.1 Study area and sampling

The Bay of Biscay is a large gulf of the Atlantic Ocean located off the western coast of France and the northern coast of Spain, between 43.5 and 48.5° N and 3 and 8° W. The principal rivers in decreasing order of drainage area are: the Loire, Garonne–Dordogne (Gironde complex), Adour, Vilaine and Charente rivers (Fig. 1). The continental shelf reaches widths of about 140 km off the coast of Brittany but narrows to less than 15 km off the Spanish shore. The physical and hydrological features of the Bay of Biscay

OSD
10, 2207–2254, 2013

are of great complexity, e.g. coastal upwelling, coastal run-off and river plumes, seasonal currents, eddies, internal waves and tidal fronts (Lavin et al., 2004). These abiotic processes greatly influence the phytoplankton dynamics and as a consequence, the whole food-web composition, structure and functioning (Varela, 1996). The samples come from the PELGAS and PELACUS cruises, French and Spanish small pelagic surveys held in spring in the Bay of Biscay on board *NO Thalassa*. At each station and at night a structure containing a CTD probe (seabird SBE19) and several sensors including an LOPC is dropped from the surface to the bottom depth (max 600 m) at 1 m s^{-1}. For some stations, a WP2 net is dropped to 100 m depth (or to the bottom for coastal stations) and towed vertically to the surface. The total numbers of stations with LOPC and/or WP2/Zs data are presented on Table 1. The dataset comprises sampling from PELGAS cruises in 2005, 2007, 2009, 2010, 2011 and 2012, and from PELACUS cruises in 2005, 2006, 2007 and 2009. The LOPC was not operated in missing years.

2.2 Measurement of the size distribution

2.2.1 Laser-Optical Plankton Counter (LOPC)

The Laser Optical Plankton Counter (Herman et al., 2004), is an optical instrument capable of measuring in situ the size of particles crossing its field by means of recording laser intensity attenuation. Smallest recorded objects are of ~ 100 µm ESD and largest are of few millimeters to centimeters. In the present work we limited the analysis to sizes below 1.9 mm ESD that corresponds to the maximum size of SEPs (MEPs lower than 1.9 mm ESD were added to the size distribution). SEPs are Single Element Particles and MEPs are Multiple Element Particles, which means that MEPs activate more than one diode when crossing the laser field of the LOPC. The LOPC takes two records per seconds and has a sampling window of 49 cm^2. Problems of coincidence in case of high particles concentration that arise often with the OPC (Woodd-Walker et al., 2000) are largely decreased with the LOPC (Herman et al., 2004). The LOPC is mounted on the CTD-Rosette and samples the water column at a rate of 2 Hz giving, at a maximal

OSD
10, 2207–2254, 2013

lowering speed of 1 m s^{-1}, a minimal vertical resolution of 0.5 m. A total of 816 LOPC casts are used in the present work (Table 1).

2.2.2 WP2 net samples and in lab imaging analysis (WP2/Zs)

Zooplankton sampling was done at night by vertical tows (100 m depth or bottom depth to surface) of a WP2 net (mesh size of 200 µm, mouth aperture of 0.25 m^2). Since no flowmeters were mounted on nets, the sampled volume was simply calculated as the maximum depth times the mouth aperture of the net. According to Nichols and Thompson (1991) a net is quantitative for objects which have a width of a minimum of 4/3 the mesh of the net (here 200 µm). Considering a minor : major axes ratio (the minor axis is here considered as a proxy of the width) of 0.45 (Vandromme et al., 2012, average for copepods) it implies that the WP2 will quantitatively sampled objects from ~ 400 µm ESD, which corresponds to the mode of the size spectra found from WP2 samples (Vandromme et al., 2012). Throught comparison with larger net, the upper size limit of quantitative sampling is ~ 2500 µm ESD (Vandromme et al., 2012). A selection of available WP2 samples representative of different locations of the area were processed with the ZooScan/ZooProcess system, a laboratory flatbed scanning system used for the digitization of fixed wet net samples developed at the Laboratory of Oceanography of Villefranche-sur-mer (Gorsky et al., 2010). Each sample was separated in two size fractions with a mesh of 1000 µm to avoid underestimation of large objects. Then, each size-fraction subsample was fractionated separately with a Motoda box. Each subsample was scanned after a manual separation of objects on the scanning tray to reduce the occurence of touching objects (Vandromme et al., 2012). The ZooScan used here had a scanning surface of 15 × 24 cm and a pixel width of 10.56 µm (scan at 2400 dpi; 14 200 × 22 700 pixels). Images are analyzed by a dedicated imaging software, ZooProcess. This software, (i) scans a high-quality raw image, linked with associated metadata, (ii) divides the raw image into separate valid targets, defined by the continuity of pixels with grey levels lower than a threshold of 243 (8 bits grayscale;

OSD
10, 2207–2254, 2013

black = 0 and white = 255), and (iii) measures 46 variables for object characterization, including grey levels, fractal dimension, shape and size (Gorsky et al., 2010). ~~Using these variables, a~~ supervised classification of objects into groups was performed consisting of a rough pre-sorting that was further visually corrected to ensure discriminating zooplankton from non-living particles. Zooplankton images from PELGAS cruises were then classified in 18 categories. A total of 89 WP2/Zs samples are used in the present work (Table 1).

2.2.3 Size spectra calculation

The size spectra are expressed as Normalized Biomass Size Spectra (NBSS) in the sense of Platt and Denman (1977) and Blanco et al. (1994)~~, i.e.~~,

$$\beta(w) = \frac{B(w)}{\Delta(w)} \quad (1)$$

where w is the carbon weight for a given size class, $\beta(w)$ is the normalized form, $B(w)$ is the unormalized form and $\Delta(w)$ is the width of each size class. The carbon weight is calculated from the ESD of each objects (both for the LOPC and the WP2/Zs) following ~~conversions~~ for general zooplankton of Lehette and Hernández-León (2009) ~~that relate ESD to dry weight and according to a dry weight to carbon ratio of 0.447 (Mauchline, 1998)~~:

$$\mathrm{ar} = \pi\ (\mathrm{ESD}/2)^2 \quad (2a)$$

$$\mathrm{dw} = 43.38\ \mathrm{ar}^{1.54} \quad (2b)$$

$$w = 0.447\ \mathrm{dw} \quad (2c)$$

ar is the projected 2-D area of the object (in mm^2), dw is the dry weight (in µg) and w is in µgC. Size spectra are displayed in logarithmic scales and a log-linear regression is performed to compute the slope (s) and the intercept (a) for each of them. The

OSD
10, 2207–2254, 2013

log-linear regression ~~was~~ made from the average mode of size spectra. While nonlinear functions usually produce a better fit to size distribution data (Gasol et al., 1991; Vidondo et al., 1997; Brucet et al., 2005), the ecological meaning of the model parameters is normally difficult to interpret (Quintana et al., 2008) and so, those nonlinear functions ~~have not been~~ applied in the present analysis.

2.3 Environmental dataset

For each station a set of hydrological parameters were extracted, using mainly measure of the CTD probe. For temperature, salinity and density ~~we used the~~ value at surface and bottom (surface ~ 4 m depth, bottom ~~corresponds~~ to 100 m or less, depending on the bathymetry). ~~We included also~~ the total fluorescence integrated from surface to bottom, the depth of the maximal fluorescence and the value of fluorescence at its maximum. Fluorescence data were calibrated each year against in situ measurements of chlorophyll *a*. ~~From density we computed the stratification (first differences) and used the mean value as well as the maximum one.~~ ~~We also included~~ the mixed layer depth ~~which is calculated by~~ a finite difference criteria method ($0.02\,kg\,m^{-2}$ more than the surface (4 m depth) value, Kara et al., 2000). In addition ~~we included~~ daily satellite data, chlorophyll *a* and inorganic Suspended Particulate Matter (SPM) processed with a specific algorithm for Case 2 coastal waters (Gohin et al., 2005)~~,~~ at the sampling date as well as 7 and 14 days before. Finally, bathymetry, distance to the coast, latitude and julian day were also included. This ~~builds~~ a total of 22 explanatory variables. Integrated and maximum fluorescence, satellite chlorophyll *a* and suspended matter as well as bathymetry were log transformed. At some stations, the surface chlorophyll *a* was measured for three size fraction, i.e. below 3 µm, from 3 to 20 µm and above 20 µm.

2.4 ~~Analysis~~

~~We are assuming that the~~ WP2/Zs estimates the size distribution of the zooplankton only ~~while~~ the LOPC estimates the size distribution of both the zooplankton and

OSD
10, 2207–2254, 2013

non-living particles (organic and ~~non-organic~~ particulate matter) and thus gives always a larger estimate than the WP2/Zs. The LOPC size spectra were first averaged over the same depth intervals as the WP2/Zs (i.e., up to 100 m or bottom depth). According to the size specificities of each sampling device (LOPC and WP2/Zs~~, see Sect. 2.2~~), the window of comparable size ~~ranges~~ from ~ 400 to 2000 µm ESD. ~~We then considered~~ the size distribution of non-living particles as the subtraction of the WP2/Zs NBSS from the LOPC NBSS on this size range. On it we performed a log-linear regression and we will consider the slope (a_{nl}) and the intercept (b_{nl}) of this regression as the descriptors of the non-living (nl) particles size distribution. ~~We can notice that~~ even if a_{nl} and b_{nl} are generally independent, in the special case of the NBSS, where biomass values are constrained by the carrying capacity of the ecosystem, some dependency exists between these two descriptors. Statistical analyses performed hereafter however took this dependency into account.

In order to assess the main factors explaining the size distribution of non-living particles we performed a Stepwise Redundancy Analysis (Stepwise RDA Legendre and Legendre, 2012, Chap. 11.1). RDA is the direct extension of multiple regression to the modelling of multivariate response data, redundancy being synonymous with explained variance. A table of explanatory variables (**Y**) is used to explain a table of responses variables (**X**). The ordination of **Y** is constrained in such a way that the resulting ordination vectors are linear combinations of the variables in **X**. Here, the table **X** corresponds to the two coefficients (a_{nl} and b_{nl}) that will be applied on the LOPC NBSS to estimate the WP2/Zs NBSS. The table **Y** is a set of explanatory variables described in Sect. 2.3 together with the NBSS LOPC derived biomass (in $\log_{10}$) and slope. A selection of explanatory variables is performed via a Stepwise RDA. Variables are sequentially added by selecting the one that yields the largest variance (partial F-statistic) and by removing it for the next selection step. Variables are thus sorted from the one that explains the most variance to the lowest.

To calculate the coefficients of the regression that estimate a_{nl} and b_{nl} we used a Partial Least Square regression (PLS regression, de Jong, 1993; Rosipal et al., 2006). PLS

OSD
10, 2207–2254, 2013

regression is used to find fundamental relations between two matrices (**X**, the table of responses variables and **Y**, the table of explanatory variables), i.e. a PLS model will depict the multidimensional direction in the **Y** space that explains the maximum multidimensional variance direction in the **X** space through computing principal components of the matrix **Y**. PLS regression are generally used when there is a large number of explanatory variables and a covariance among them. The robustness of the PLS regression was assessed by performing a total of 5000 permutations with a random removal of 4 stations for each permutation. Average PLS regression coefficients are then applied on the whole LOPC size spectra to estimate the zooplankton size distribution for each station of each year occuring in the dataset. These steps are shown on Fig. 2.

Further, the zooplankton ~~estimated~~ productivity ~~is calculated by using the formulation of Zhou et al. (2010)~~ based on the model of Huntley and Boyd (1984) and Hirst and Bunker (2003)~~. The~~ growth of zooplankton is a function of water temperature, chlorophyll *a* and weight of individuals (in mg C)~~. The~~ production is the growth rate ~~multiply~~ by the total biomass of zooplankton~~. The~~ total biomass is calculated as the integral of an assumed linear NBSS:

$$B = \int_{x_{min}}^{x_{max}} a x^s \, \mathrm{d}x \tag{3a}$$

$$B = \frac{a {x_{max}}^{s+1}}{s+1} - \frac{a {x_{min}}^{s+1}}{s+1} \tag{3b}$$

where B is the biomass between x_{min} and x_{max} ~~and~~ s is the slope and a the intercept of the NBSS. ~~Here,~~ x_{min} ~~corresponds to 200 µm ESD~~ and x_{max} corresponds~~s~~ to 2000 µm ESD, ~~which cover~~ the size range of the meso-zooplankton. ~~the~~ production is summed from the surface to a max of 100 m depth to have an estimated productivity per square meter.

Maps of zooplankton estimated biomass, slopes and productivity ~~are~~ computed for each year on a 50 × 50 grid (~ 20 × 20 km cells) covering the whole Bay of Biscay. Val-

OSD
10, 2207–2254, 2013

ues at nodes ~~are~~ computed as the average ~~of values~~ in a radius of 30 km weighted by the inverse of the squared distance. Climatological maps is then calculated by taking the mean of each annual map of zooplankton biomass, slopes and productivity. The ~~biomass of~~ zooplankton ~~is~~ presented both as the average concentration, in mg C m^{-3}, from the surface to the bottom or to 100 m depth and as the integrated value, in mg C m^{-2}~~,~~ ~~from the surface to the bottom or to 100 m depth~~. Maps of standard deviation and number of years with value at each node ~~are~~ also presented.

In the last part, 5 groups are isolated by means of *K* means clustering computed on normed values of slopes and log-transformed biomass. The number of groups ~~is arbitrary and was choosen~~ as the best trade-off between the level of details needed to detect patterns and lisibility. The inter-annual and spatial variability of these groups is further investigated.

All analysis were performed with Matlab R2012a (The Mathworks) with the use of the statistics toolbox ~~(The Mathworks)~~ and the Fathom toolbox for the Stepwise RDA (maintained by David L. Jones, www.marine.usf.edu/user/djones).

3 Results

3.1 Size distribution of non-living particles

The LOPC size spectra ~~averaged from surface to 100 m depth (or bottom depth)~~ ~~show~~ slopes ranging from −1.73 to 0.40 ~~among all 816 stations~~, with a mean of −0.97 ± 0.24 (of standard deviation). Intercepts ~~range~~ from −1.88 to 5.15 with a mean of 1.76 ± 1.39. The coefficients of determination against the linear regression ~~shows~~ a mean of 0.95 ± 0.03 highlighting the high linearity of the size distribution. WP2/Zs size spectra show slopes ranging from −2.08 to 0.10 with a mean of −0.86 ± 0.40, and intercepts ranging from −2.36 to 2.54 with a mean of 0.15 ± 1.20. The coefficients of determination of WP2/Zs size spectra against the linear regression were 0.92 ± 0.06, slightly less than LOPC size spectra. LOPC and WP2/Zs slopes have a Pearson correlation coefficient of

OSD
10, 2207–2254, 2013

0.57 and their intercepts of 0.62. On Fig. 3 ~~various~~ examples of LOPC and WP2/Zs size spectra measured at same stations are presented. ~~Examples include an overestimation by the LOPC for each size (Fig. 3a), an overestimation for lower size only (Fig. 3b) and no differences between both spectra (Fig. 3c).~~ The first case corresponds to a larger LOPC intercept but no difference in the slope estimate, in the second case the LOPC intercept is larger and its slope is steeper than of the WP2/Zs, then in the third case no difference exist in the intercept and slope of both. Differences ~~in~~ slope and intercepts ~~for all the 89 stations are shown on Fig. 4. It corresponds to intercepts and slopes~~ of the size distribution of non-living particles within this size range. For some cases, the slope of the WP2/Zs was steeper than that of the LOPC (red colored), however, the WP2/Zs never overestimated the LOPC in the present dataset. These cases appear in PELGAS 2009 and 2010 and ~~are~~ mainly located on very coastal stations. Stations were both devices estimate are comparable (small white circles) are generally located off-shore in the middle of the continental shelf or over the slope of the French slope. For other cases, no geographical pattern clearly emerged. During PELGAS 2011 (Fig. 4e) non-living particles seem mainly distributed in the southern part of the French continental shelf~~, yet, this was not the case for other years~~.

~~To depict the main variables (**Y** matrix) affecting the size structure of non-living particles (**X** matrix) we performed a~~ stepwise Redundancy Analysis ~~(RDA, see Sect. 2.4)~~, results are shown in Table 2. The cumulative explained variance (Cum. Exp.) for all variables included reaches 73 % of the total variance of non-living particles slopes and intercepts. ~~The variable that explains the~~ most variance is the total biomass of particles in the water column estimated from LOPC (40 % of variance explained), followed by the chlorophyll *a* measured by satellite at the sampling time (52 % Cum. Exp.), the bathymetry (56 % Cum. Exp.) and the slopes of the size distribution of all particles measured with the LOPC (59 % Cum. Exp.). Since the variance explained by a variable is removed prior to the selection of the next variable, a variable strongly correlated with a previous extracted one is not likely to add a lot of cumulated explained variance. The variance explained by each variable on the initial **X** matrix is shown in the column Tot.

OSD
10, 2207–2254, 2013

Expl. of the Table 2. For example, the julian day explains 12 % of the initial **X** matrix but appears on the 9th position in the stepwise RDA and add only 1 % to the cumulative explained variance.

To further depicts variables explaining the variance of the non-living particles size distribution we added supplementary variables that were available only for some stations, thus we worked on a reduce dataset. ~~The~~ Table 3 shows the effect of including fractionated surface chlorophyll *a* to the **Y** matrix. The chlorophyll *a* was measured for the fraction below 3 µm (chlorophyll *a* 1), then from 3 to 20 µm (chlorophyll *a* 2), and above 20 µm (chlorophyll *a* 3). A total of 68 stations (among the 89) were available and belong to PELGAS 2009, 2010 and 2011. On these ~~68~~ stations the total cumulated explained variance without fractionated chlorophyll *a* is 74 % and reaches 80 % with it. The first variable to be extracted is, as above, the LOPC derived biomass (41 % Cum. Exp.) followed by the chlorophyll *a* in the larger size class (51 % Cum. Exp.), the bathymetry (56 % Cum. Exp.) and the chlorophyll *a* in the second size class (59 % Cum. Exp.). This first four variables accounts for the same explained variance as the first four above (Table 2). A last stepwise RDA was done, using taxonomic data (total of 18 zooplankton categories) from the WP2/Zs (75 stations belonging to PELGAS 2009, 2010 and 2011). Results are shown on Table 4. The stepwise RDA with same explanatory variables as above (Table 2) shows a total cumulated explained variance of 71 %, whereas all the 18 zooplankton categories explain a total of 92 % of the variance. The first four zooplankton categories explains 82 % of the variance (*Acartia* sp., cladocerans, *Calanus* sp. and other calanoids smaller than 1 mm length, see Table 4).

3.2 Accuracy of estimated zooplankton size-spectra

Using explanatory variables we estimated the size distribution of the zooplankton from size spectra measured with the LOPC, i.e., we removed the non-living part from LOPC size-spectra to approach size-spectra measured with the WP2/Zs that are assumed to represent the best estimate of the zooplankton size distribution. For that purpose we performed a Partial Least Square (PLS) regression (see Sect. 2.4) of the explanatory

OSD
10, 2207–2254, 2013

variables (matrix **Y**) on the response matrix (**X**). For the 5000 permutations performed the average explained variance was of 74.7 ± 1.9 %, similar to the the stepwise RDA. Estimated parameters of the non-living particles size spectra were then subtracted to the initial LOPC size spectra (hereafter, LOPC) to obtain the estimation of the zooplankton size spectra (hereafter, PLS reg.). Correlations between WP2/Zs slopes and intercepts and LOPC ones before and after the subtraction of non-living particles are shown on Fig. 5 and on Taylor diagrams (Fig. 6, Taylor, 2001). The Pearson correlation between WP2/Zs slopes and intercepts with the ones of the LOPC are respectively of 0.57 ($p < 0.001$) and 0.62 ($p < 0.001$). In the case of the intercepts (Fig. 5b) a strong overestimation by the LOPC is also observed. After the subtraction, Pearson correlations reach 0.78 and 0.85 (both $p < 0.001$) for slopes and intercepts respectively. The overestimation of the intercept by the LOPC is reduced with the PLS reg. ~~This is clearly seen on the Taylor diagram~~ (Fig. 6b).

WP2/Zs slopes (s) and intercepts (a) are significantly correlated (Pearson $r = -0.86$, $p < 0.001$) and related by a linear fit on the form $a = p_1 s + p_2$ where $p_1 = -2.568(-2.895, -2.241)$ and $p_2 = -2.062(-2.372, -1.752)$, numbers in parenthesis indicate the 95 % confidence interval. For the LOPC, the Pearson correlation is of -0.70 ($p < 0.001$) and the linear fit has coefficients $p_1 = -4.144(-4.445, -3.842)$ and $p_2 = -2.251(-2.551, -1.951)$. Slopes and intercepts estimated by the PLS regression are also significantly correlated (Pearson $r = -0.84$, $p < 0.001$) and have coefficients $p_1 = -3.181(-3.331, -3.031)$ and $p_2 = -2.606(-2.727, -2.486)$. These correlations are shown on Fig. 7. The subtraction of non-living particles tends to reproduce the initial correlation that exists between slopes and intercepts of the zooplankton size spectra.

3.3 Spatial and inter-annual distribution of zooplankton

On Fig. 7 the estimated biomass computed as the integral of a linear NBSS defined by its slope and intercept is displayed as a color scale in $\log_{10}$. The strength of the relation between biomass and size spectra parameters is affected by the position of the

OSD
10, 2207–2254, 2013

subset slopes vs. intercepts. For the values of slopes and intercepts observed here we have a Pearson correlation of biomass and slopes of −0.51 ($p < 0.001$), the relation is displayed on Fig. 11: $\log_{10}(B) = -0.571s + 0.544$. The estimated zooplankton biomass concentrations range from 2.9 to 63.7 mg C m^{-3} with a mean of 11.4 ± 8.2 mg C m^{-3} (median of 8.9 mg C m^{-3}). The depth integrated zooplankton biomass ranges from 37.7 to 4614.5 mg C m^{-2} with a mean of 804.2 ± 421.0 mg C m^{-2} (median of 753.6 mg C m^{-2}). A general tendency of large biomass associated with steeper size spectra is observed. This tendency also emerged from climatological maps (Figs. 8, 9 and 10) where maximum values of biomass are observed near the coast of the northern part of the Bay of Biscay (especially off the Vilaine estuary) and on the coast of Galicia which roughly corresponds to the steepest slopes observed. Lowest biomass values are observed on average in the southern part of the Bay, in the Cap Breton area and off Portugal. Low values occur also throughout the French continental shelf. In term of biomass, one of the most variable area observed is the Gironde plume (Fig. 8c).

The inter-annual and spatial patterns were investigated through the 5 groups identified by the *K* means clustering based on estimated slopes and biomass of the zooplankton (Fig. 11). Annual and spatial distribution of these groups is shown in Fig. 12. The first group (blue circles) corresponds to largest biomasses concentration (median of 32 ± 11.8 mg C m^{-3}) and steepest size spectra (median of −1.19 ± 0.14). This group is almost exclusively found in the most coastal areas, notably in the main estuaries of the french coast (Gironde, Charente, Loire, Vilaine) but also in the coastal area south of the Gironde estuary (the Landes), in the coast of western Brittany and along the Galician coast. An important inter-annual variability is observed with the quasi absence of this group during the spring of 2011 compared to springs of 2009 and 2010, the two years with the most occurence of this group. The second group (green squares) shows the second largest biomass concentration (median of 15.9 ± 5.2 mg C m^{-3}) and second steepest size spectra (median of −0.94 ± 0.13). This group occurs, as group 1, mainly in coastal areas, although it extends more over the plateau. This group shows less inter-annual variability than the first one with, yet, a higher occurence during spring 2011,

OSD
10, 2207–2254, 2013

notably in estuarine areas. The third group (red losanges) has a median biomass concentration of $7.9 \pm 1.5\,mg\,C\,m^{-3}$ and slopes of -0.83 ± 0.10. In 2005 and 2007 this group is observed mainly in the ~~s~~panish and ~~p~~ortugese coasts, while, from 2009, many occurence of this group were observed further north, specifically in the Cap-Breton area (~~south east of the bay~~), mid-plateau and continental slope. The forth group (black triangles) has the lowest biomass concentration (median of $4.9 \pm 1.0\,mg\,C\,m^{-3}$) and second flatest size spectra (median of -0.66 ± 0.10). As the latter group, the forth group is mainly observed at southern location (Cantabrian sea and portugese slope) in 2005, 2006 and 2007. In 2005, this group was also observed in the Cap-Breton area. From 2009, an extension northward is observed with many occurence in the french slope and off the Cap-Breton. In 2012, this group is also observed mid-plateau up to Brittany. The last group (pink stars) has biomass concentrations of $9.5 \pm 2.5\,mg\,C\,m^{-3}$ and the flatest size spectra (median of -0.55 ± 0.10). This group is the most off-shore, with most occurence mid-plateau and at the slope. This group was also observed, mainly in 2007, in the ~~s~~panish coast. In 2009 and 2010, stations close to the Gironde estuary belonging to this group were recorded. In 2012 this group was also observed at some locations along the Brittany coast.

3.4 Zooplankton productivity

The productivity of zooplankton, ~~in term of $mg\,C\,m^{-2}\,d^{-1}$, was computed using a model based on the size of the zooplankton, water temperature and chlorophyll *a* (see Sect. 2.4). Estimates~~ ranged from 0.0011 to $0.58\,mg\,C\,m^{-2}\,d^{-1}$, with a mean of 0.036 ± 0.050 and a median of $0.021\,mg\,C\,m^{-2}\,d^{-1}$. The climatological map of zooplankton productivity~~, calculated as for Figs. 8 and 10,~~ is presented on Fig. 13. ~~On average, the less productive area, but also the most variable, is the area off Cap Breton and the eastern coast of the Cantabrian Sea. Most productive area are the river plume of Gironde and Loire/Vilaine, but also the French continental slope followed by the Galician area.~~

OSD
10, 2207–2254, 2013

4 Discussion

4.1 A large scale homogeneous sampling

Several studies aim to compare efficiency of sampling methodologies in providing size structure of mesozooplankton, among them LOPC and net tow combined with identification or image analysis (Nogueira et al., 2004; Schultes and Lopes, 2009). ~~Here we took~~ advantage of both methodologies, taxa resolution of the zooscan with conveniency of the LOPC to provide homogeneous size structure information at the scale of the Bay of Biscay shelf. French Pelgas survey directly follows spanish Pelacus survey aboard the same vessel, and both operate similar LOPC and WP2 net tows. This limits sources of errors from sampling differences when further comparing spatial variability over this large area. However this also means a large difference between starting date of first survey in the south and end of second one in the north (~ 2 months). This potentially bias the interpretation we make on spatial variability, which encompass seasonal evolution, especially during the spring season when rapid changes in the environment occurs (Koutsikopoulos et al., 1996). This effect is partly mediated since the productive season progresses from south to north following temperature and stratification increases (Koutsikopoulos et al., 1996), which has the effect of attenuating differences arising from seasonality. In addition, the repeatability across years of spatial patterns when looking at NBSS slope with low standard deviation, or habitat classification from clustering, especially over the Frensh shelf for which more years are available, provide arguments for considering our climatologies as robust in representing the spring situation.

The sampling strategy of the survey prevents any assessment of observed variability at short temporal (Sourisseau and Carlotti, 2006) and spatial scale, while interpretation may be affected by population dynamic patterns or patchiness. However, as noticed by Sourisseau and Carlotti (2006), the spatial variability at our sampling scale is higher than the temporal variability, giving confidence to our results. Distance between stations are approximately 24 nm (~ 44 km) in the alongshore direction, and 10 to 25 nm (~ 19

OSD
10, 2207–2254, 2013

to 46 km) in the cross-shelf direction which shows strongest gradients, with refinement for the latter in the known frontal areas and over the Iberian shelf. Based on analysis of Albaina and Irigoien (2004), a minimum resolution of 12 nm (~ 22 km) is necessary in the cross-shelf direction to obtain realistic patterns of mesozooplankton distribution, thus our sampling should allow identification of major spatial patterns of size distribution and habitat at mesoscale.

Non-linearity of the size spectrum is a common observed feature (Nogueira et al., 2004; Sourisseau and Carlotti, 2006) and reflects a non equilibrium state as compared to theoretical models (Kerr and Dickie, 2001). However, two arguments were in favour of using a linear regression model to calculate the NBSS. First we found high coefficients of determination for the adjusted models at each station and for both instruments. Second, in our study and with our low temporal resolution data we are more interested here at looking at principal scalings of the ecosystem structure (zooplankton size spectrum and its spatial variability, Kerr and Dickie, 2001), that is physiological (primary scaling) and ecological (secondary scaling), rather than short term population dynamics, one of the factor leading to these non-linearities. The linearisation of the measured spectrum in our analysis, as well as presentation of results through climatologies tends to filter out the short spatio-temporal variability.

4.2 Correction of the size spectra

To separate living and non-living particles counted by the LOPC we use a direct comparison with net catches performed at the same position and at the same time. The statistical correction was made only on the common valid part of the size spectrum for each instrument (~ 400 to 2000 µm ESD), to reduce uncertainties arising from undersampling at lower and upper limits of the mesozooplankton size range. Differences between both spectra were assumed to originate from non-living particulate matter. LOPC counts were, within the present dataset, always higher or equal to the WP2/Zs counts giving weight to the assumption that the LOPC accurately counts both living and non-living particles. Properties of this difference (slope and intercept of the log-linear

OSD
10, 2207–2254, 2013

regression) were related to the ones of the LOPC size spectra and to the environmental variables. The resulting multiple regression was further used to estimate the size distribution of non-living particles at location where only LOPC data are available.

In the present work, the correction significantly improved the reliability of the LOPC-derived NBSS, both in terms of correlation with the WP2/Zs-derived NBSS, and of properties of the NBSS, i.e. correlation between slope and intercept. Remaining unexplained variability may have several of the following origins difficult to further assess from our study: (i) the lacking information included in the explanatory environmental variables, as well as the associated errors associated to their measurement, (ii) errors from various origin in the estimation of volume sampled by the net (Nogueira et al., 2004; González-Quirós and Checkley, 2006; Schultes and Lopes, 2009) as well as further fractioning before Zooscan processing, and (iii) various efficiency between instruments especially at the tails of the size range even if caution was taken in its selection, with potential avoidance of larger individuals.

4.3 Interpretation of the correction

Our correction methodology from the LOPC NBSS towards the WP2/Zs NBSS makes best use of available environmental information, both in situ and satellite. One could think of direct statistical models to estimate the correct NBSS properties and propose some extrapolation for periods without sampling. But the occurence of LOPC-derived biomass, and to a lesser extent of the LOPC slope, in first positions of the explanatory variables (Tables 2 and 3) for the differences between spectrum properties give strong interest of using the LOPC despite its contamination by non-living particles.

In addition to the uncorrected NBSS properties, chlorophyll (either from satellite, Table 2, or as fractionated measurements, Table 3) appears as the second explanatory variable. This confirms that the majority of the difference between both instruments is due to particulate organic matter, being highest in areas with detrital products of large phytoplankton blooms (fractions higher than 30 µm) or associated zooplankton blooms. Looking only at satellite-derived chlorophyll, highest variability is explained by one week

OSD
10, 2207–2254, 2013

past situation (4.47 %), again highlighting the potential role of past bloom in detritus concentration, even if in the stepwise RDA current chlorophyll situation takes priority. In opposition, inorganic SPM from satellite does not explain much variability, their small size being unavailable to both type of measurements. Julian day, taken separately, explains more than 10 % of the variability. This may be explained also by the timing of sampling with respect to bloom phenology, with highest detritus concentrations in post-bloom conditions later in spring. Non-living particulate material may also ~~has~~ terrestrial or resuspension origin, which ~~is~~ reflected in the salinity or distance to coast covariables, but here again redundancy with other variables (likely with bathymetry ~~but also~~ coast-to-offshore gradient of the size spectra) prevent them to be at the top of the list of the cumulated explained variance.

Interestingly, using taxonomy information, we successfully explained a larger part of the correction variability. Size structure is implicitly considered by the abundance of each taxa, but in addition this reveals that taxonomy also implicitly introduce spatial information such as distance from coast with community structuration along a cross-shore gradient (Albaina and Irigoien, 2004), likely some information on phenology and succession of plankton species, and finally some information on quantity and quality of associated detrital matter. In case ~~that living~~ fragile particles such as gelatinous zooplankton ~~are also~~ part of the difference between both instrument measurements, ~~then~~ taxonomy information may also bring some information on the community assemblages not explained by other covariables. This latter analysis with taxonomy was mainly exploratory since no simultaneous information is available for systematic correction, ~~but~~ this motivates the effort to be set on further development of in situ imaging system.

4.4 Size spectrum patterns

The estimated mesozooplankton biomass (2.9 to 63.7 mg C m^{-3}) is in agreement with values reviewed by Poulet et al. (1996) in the area, or with high resolution sampling in spring over the southern shelf of the Bay by Irigoien et al. (2009). The slopes of the NBSS range from −1.4 to −0.2 with a mean of −0.8 slightly flatter that the commonly

OSD
10, 2207–2254, 2013

accepted slope of −1 typical of steady-state large ecosystems (Platt and Denman, 1977; Kerr and Dickie, 2001) ~~indicating~~ a small : large ratio in favor of larger individuals, most likely explained by the post-bloom conditions. ~~Spatial distribution of size structure as~~ climatology confirms the remarkable positive coast to off-shore gradient of the NBSS slope, with a slight decrease when reaching the shelf break, especially over the french shelf in coherence with observations by Sourisseau and Carlotti (2006) and Irigoien et al. (2009). We do not observe an opposite gradient over the North Iberian shelf, as clearly appeared from observations by Nogueira et al. (2004) during winter to spring transition in 2002, but we observe their west to east trend of steeper to flatter slopes. ~~Fewer~~ years ~~are~~ available to built a robust climatology in that area.

From 5 yr and high resolution sampling over a transect offshore the Gironde estuary, Albaina and Irigoien (2004) described the following structuration for the mesozooplankton community: (i) a river plume area with high abundance of small individuals, (ii) a shelf break frontal zone with relatively high abundance, (iii) the shelf zone with much lower abundance but large species, and (iv) an oceanic zone. Apart from the latter that is not well sampled in our surveys except for 2011 and 2012 in the south (Fig. 12), our results show a similar cross-shelf structure over the whole area north of the Gironde. Indeed, the coastal zone shows steeper slopes from a large proportion of small individuals, mid-shelf zone has flattest slopes with highest relative proportion of large individuals, and the slope then gets steeper over the shelf break.

Despite this size spectrum gradient, the biomass is relatively homogeneous as also observed by Albaina and Irigoien (2004), with only a slight decrease in the mid-shelf area and a really coastal strip of higher biomass north of the Gironde until Brittany. The bigger size of individuals in the mid-shelf area tend to compensate the fewer abundance. The absence of cross-shelf structuration in the ~~s~~outh of the ~~bay~~ and over the Iberian shelf is certainly due to the absence of the mid-shelf habitat (low occurence of group 5, see Fig. 12) with no transition between coastal and shelf break habitats. Large continental inputs along the coast and internal waves breakdown (Pingree et al., 1981) over the continental slope are stong drivers of the ecosystem dynamics over the

OSD
10, 2207–2254, 2013

French northern shelf. Those processes are lacking or really limited over the Iberian shelf which consequently shows higher spatio-temporal variability across years.

4.5 Productivity and trophic control

The integrated mesozooplankton productivity gives a significantly different picture than the biomass. The high biomass areas such as along the French and Galician coasts still appear as highly productive, but in addition the shelf slope is also quite productive when compared to the mid-shelf, which is more conspicuous again over the french shelf. This is partly due to bathymetry which tend to lower the values in coastal areas after vertical integration as compared to offshore deeper waters, but this is also explained by differences in size structure of the zooplankton and potentially primary production. The mid-shelf, with flattest slopes of the bay and large zooplankton, is estimated as less productive even if the biomass seems close to the one over the slope. This region is often rapidly and strongly stratified in spring (Koutsikopoulos et al., 1996) with low primary production limited to the thermocline after the spring bloom, and has water masses with long residence time under low residual circulation (Charria et al., 2013). In opposition, coastal areas are continuously under the influence of rich river inputs, and the slope frontal structure regularly receives nutrient inputs from breakdown of internal waves.

Variation of the slope of the size spectrum around the theoretical value of −1 typical of steady-state large ecosystems (Kerr and Dickie, 2001) has ecological significance. At the scale of our defined habitats, the slope is the result of local structuration of the community, informing on efficiency of the transfer of matter across trophic levels or type of trophic control (Suthers et al., 2006). From a litterature review, Daewel et al. (2013) could not find evidence of top-down control on zooplankton at the scale of the Bay of Biscay, even if at local scale and for particular season this can not be excluded. Steeper slopes are generally related to lower efficiency of the matter flux, potentially with top-down control, while flatter slopes areas represent efficient transfer under bottom-up control. So even if more productive, coastal areas (especially plumes) and to a lesser

OSD
10, 2207–2254, 2013

extent shelf break habitats, may have low transfer efficiency, while mid-shelf area may have high transfer efficiency through the zooplankton size range. The fact that similar ranges of biomass occur in the mid-shelf and over the slope despite higher productivity over the slope ~~is~~ a sign of higher efficiency for the mid-shelf habitat. There are usually low fish occurence in that habitat in spring during the small pelagic survey, which has the effect of releasing predation pressure on large zooplankton that would have their biomass rapidly declining otherwise. In opposition, the southeastern ~~bay~~ have high fish occurence, which could explain the lower observed biomass than in the north under top-down control.

5 Conclusions

The LOPC has been operated in the Bay of Biscay since 2005 during Spanish and French small pelagic surveys. Considering that fewer stations are sampled with net due to time constraint, and the considerable amount of lab work for taxon identification or/and size measurements (more than 1 month for scanning and classification from our 76 analysed samples from Pelgas) which often prevents complete analysis of the full set of sampled stations (here 874), the LOPC combined with our methodology provides a robust and rapid access (potentially at the end of a survey) to key information on the size structure of the mesozooplankton. ~~Further investigations of~~ selected samples may then be further analysed with binocular or ~~Zooscan~~. ~~Alternatively, in situ imaging instruments such as the UVP (Stemmann et al., 2008) can provide both size structure and taxonomy rapidly during a survey. The UVP was tested in the Bay of Biscay but the instrument would need further development for its full efficiency in loaded coastal areas.~~

Combining biomass from biogeochemical model results and size spectrum observation is an investigated approach to estimate available fraction of the total biomass to upper trophic levels (Daewel et al., 2013). The significant but relatively weak correlation between slope and biomass (Fig. 7) obtained over the whole domain does not permit

OSD
10, 2207–2254, 2013

a direct estimation of this fraction from only model biomass. Alternatively, combining model results and our NBSS slope climatology can provide a first estimation. Temporal stability of the maps of size structure presented in this study has to be verified before this approach is generalised for estimation over the whole year.

Even if able to provide abundance and biomass on lower size classes with more efficiency than the WP2 mounted with a mesh of 200 µm, the LOPC is not efficient for the microplankton size classes, also key in the energy transfer to upper trophic level, in particular as food for fish larvae. Nogueira et al. (2004) showed some continuity between the size spectra obtained from a 20 µm net and an in situ OPC. However this has to be verified over a larger set of stations before any extrapolation to be proposed from the LOPC-derived size spectra. No in situ instrument currently exist for this size range, however, the Flowcam (Fluid Imaging Technologies), operational on-board, may provide rapidly key additional information.

Acknowledgements. We are grateful to the R/V *Thalassa* crew, and to J. Massé for coordinating the Pelgas surveys over the last decade. We also thank B. Planque for initiating the use of the LOPC on PELGAS survey, and to E. Antajan for helping us with the use of the ZooScan. We also want to greatly thanks Frédéric Ibañez who introduce some of us to the world of statistics and sadly passed away recently. P. V. fellowship was founded by the project REPROdUCE of the ERA-NET MARIFISH (Contract ERAC, CT-2006-025989) and french National Research Agency (ANR).

The service charges for this open access publication have been covered by a Research Centre of the Helmholtz Association.

References

Albaina, A. and Irigoien, X.: Relationships between frontal structures and zooplankton communities along a cross-shelf transect in the Bay of Biscay (1995 to 2003), Mar. Ecol.-Prog. Ser., 284, 65–75, doi:10.3354/meps284065, 2004. 2211, 2226, 2228, 2229

OSD
10, 2207–2254, 2013

Baird, M. E. and Suthers, I. M.: A size-resolved pelagic ecosystem model, Ecol. Model., 203, 185–203, doi:10.1016/j.ecolmodel.2006.11.025, 2007. 2210

Barnes, C., Irigoien, X., De Oliveira, J. A. A., Maxwell, D., and Jennings, S.: Predicting marine phytoplankton community size structure from empirical relationships with remotely sensed variables, J. Plankton Res., 33, 13–24, doi:10.1093/plankt/fbq088, 2011. 2209

Blanco, J., Echevarría, F., and Garcia, C. M.: Dealing with size-spectra: some conceptual and mathematical problems, Sci. Mar., 58, 17–29, 1994. 2215

Brucet, S., Boix, D., Lopez-Flores, R., Badosa, A., Moreno-Amich, R., and Quintana, X. D.: Zooplankton structure and dynamics in permanent and temporary Mediterranean salt marshes: taxon-based and size-based approaches, Arch. Hydrobiol., 162, 535–555, doi:10.1127/0003-9136/2005/0162-0535, 2005. 2216

Charria, G., Lazure, P., Le Cann, B., Serpette, A., Reverdin, G., Louazel, S., Batifoulier, F., Dumas, F., Pichon, A., and Morel, Y.: Surface layer circulation derived from Lagrangian drifters in the Bay of Biscay, J. Marine Syst., 109–110, S60–S76, doi:10.1016/j.jmarsys.2011.09.015, 2013. 2230

Checkley Jr, D., Davis, R., Herman, A., Jackson, G., Beanlands, B., and Regier, L.: Assessing plankton and other particles in situ with the SOLOPC, Limnol. Oceanogr., 53, 2123–2136, doi:10.4319/lo.2008.53.5_part_2.2123, 2008. 2210

Daewel, U., Peck, M. A., Kühn, W., St. John, M. A., Alekseeva, I., and Schrum, C.: Coupling ecosystem and individual-based models to simulate the influence of environmental variability on potential growth and survival of larval sprat (*Sprattus sprattus* L.) in the North Sea, Fish. Oceanogr., 17, 333–351, doi:10.1111/j.1365-2419.2008.00482.x, 2008. 2210

Daewel, U., Hjollo, S. S., Huret, M., Ji, R., Maar, M., Niiranen, S., Travers-Trolet, M., Peck, M. A., and van de Wolfshaar, K. E.: Predation control of zooplankton dynamics: a review of observations and models, ICES J. Mar. Sci., doi:10.1093/icesjms/fst125, 2013. 2210, 2230, 2231

de Jong, S.: SIMPLS: an alternative approach to partial least squares regression, Chemometr. Intell. Lab., 18, 251–263, doi:10.1016/0169-7439(93)85002-X, 1993. 2217

Gaardsted, F., Tande, K. S., and Basedow, S. L.: Measuring copepod abundance in deep-water winter habitats in the NE Norwegian Sea: intercomparison of results from laser optical plankton counter and multinet, Fish. Oceanogr., 19, 480–492, doi:10.1111/j.1365-2419.2010.00558.x, 2010. 2211

OSD
10, 2207–2254, 2013

Gasol, J. M., Guerrero, R., and Pedrosalio, C.: Seasonal-variations in size structure and prokaryotic dominance in sulfurous lake Ciso, Limnol. Oceanogr., 36, 860–872, doi:10.4319/lo.1991.36.5.0860, 1991. 2216

Glazier, D. S.: Beyond the "3/4-power law": variation in the intra- and interspecific scaling of metabolic rate in animals., Biol. Rev., 80, 611–662, doi:10.1017/S1464793105006834, 2005. 2209

Gohin, F., Loyer, S., Lunven, M., Labry, C., Froidefond, J., Delmas, D., Huret, M., and Herbland, A.: Satellite-derived parameters for biological modelling in coastal waters: illustration over the eastern continental shelf of the Bay of Biscay, Remote Sens. Environ., 95, 29–46, doi:10.1016/j.rse.2004.11.007, 2005. 2216

González-Quirós, R., and Checkley, D. M.: Occurrence of fragile particles inferred from optical plankton counters used in situ and to analyze net samples collected simultaneously, J. Geophys. Res., 111, C05S06, doi:10.1029/2005JC003084, 2006. 2211, 2227

Gorsky, G., Ohman, M. D., Picheral, M., Gasparini, S., Stemmann, L., Romagnan, J.-B., Cawood, A., Pesant, S., Garcia-Comas, C., and Prejger, F.: Digital zooplankton image analysis using the ZooScan integrated system, J. Plankton Res., 32, 285–303, doi:10.1093/plankt/fbp124, 2010. 2211, 2214, 2215

Herman, A. W. W., Beanlands, B., and Phillips, E. F. F.: The next generation of Optical Plankton Counter: the Laser-OPC, J. Plankton Res., 26, 1135–1145, doi:10.1093/plankt/fbh095, 2004. 2210, 2211, 2213

Hirst, A. G. and Bunker, A. J.: Growth of marine planktonic copepods: global rates and patterns in relation to chlorophyll *a*, temperature, and body weight, Limnol. Oceanogr., 48, 1988–2010, doi:10.4319/lo.2003.48.5.1988, 2003. 2218

Huntley, M. and Boyd, C.: Food-limited growth of marine zooplankton, Am. Nat., 124, 455–478, doi:10.1086/284288, 1984. 2218

Irigoien, X., Fernandes, J. A., Grosjean, P., Denis, K., Albaina, A., and Santos, M.: Spring zooplankton distribution in the Bay of Biscay from 1998 to 2006 in relation with anchovy recruitment, J. Plankton Res., 31, 1–17, doi:10.1093/plankt/fbn096, 2009. 2211, 2228, 2229

Kara, A. B., Rochford, P. A., and Hurlburt, H. E.: An optimal definition for ocean mixed layer depth, J. Geophys. Res.-Oceans, 105, 16803–16821, doi:10.1029/2000JC900072, 2000. 2216

Kerr, S. R. and Dickie, L. M.: The Biomass Spectrum: A Predator-Prey Theory of Aquatic Production, Columbia University Press, 2001. 2226, 2229, 2230

OSD
10, 2207–2254, 2013

Koutsikopoulos, C., Le Cann, B., and Cann, B. L. E.: Physical processes and hydrological structures related to the Bay of Biscay anchovy, Sci. Mar., 60, 9–19, 1996. 2225, 2230

Krupica, K. L., Sprules, W. G., and Herman, A. W.: The utility of body size indices derived from optical plankton counter data for the characterization of marine zooplankton assemblages, Cont. Shelf. Res., 36, 29–40, doi:10.1016/j.csr.2012.01.008, 2012. 2210

~~Lavin, A., Valdes, L., Sanchez, F., Abaunza, P., Forest, A., Boucher, J., Lazure, P., and Jegou, A.-M.: The Bay of Biscay: the encountering of the ocean and the shelf (18b, E), in: The Sea, Vol. 14, 933–1002, 2004. 2213~~

Legendre, P. and Legendre, L.: Numerical Ecology, 3rd edn., Elsevier, Amsterdam, 2012. 2217

Lehette, P., and Hernández-León, S.: Zooplankton biomass estimation from digitized images: a comparison between subtropical and Antarctic organisms, Limnol. Oceanogr.-Meth., 7, 304–308, doi:10.4319/lom.2009.7.304, 2009. 2215

Mauchline, J.: The biology of calanoid copepods, Adv. Mar. Biol., 33, 1–710, 1998. 2215

Morote, E., Olivar, M. P., Villate, F., and Uriarte, I.: A comparison of anchovy (Engraulis encrasicolus) and sardine (Sardina pilchardus) larvae feeding in the Northwest Mediterranean: influence of prey availability and ontogeny, ICES J. Mar. Sci., 67, 897–908, doi:10.1093/icesjms/fsp302, 2010. 2210

Nichols, J. H. and Thompson, A. B.: Mesh Selection of Copepodite and Nauplius Stages of 4 Calanoid Copepod Species, J. Plankton Res., 13, 661–671, 1991. 2211, 2214

Nogueira, E., González-Nuevo, G., Bode, A., Varela, M., Morán, X. A. G., and Valdés, L.: Comparison of biomass and size spectra derived from optical plankton counter data and net samples: application to the assessment of mesoplankton distribution along the Northwest and North Iberian Shelf, ICES J. Mar. Sci., 61, 508–517, doi:10.1016/j.icesjms.2004.03.018, 2004. 2211, 2225, 2226, 2227, 2229, 2232

Peters, R. H. and Wassenberg, K.: The Effect of body size on animal abundance, Oecologia, 60, 89–96, doi:10.1007/BF00379325, 1983. 2209

Petrik, C. M., Jackson, G. A., and Checkley, D. M.: Aggregates and their distributions determined from LOPC observations made using an autonomous profiling float, Deep-Sea Res. Pt. I, 74, 64–81, doi:10.1016/j.dsr.2012.12.009, 2013. 2210

Picheral, M., Guidi, L., Stemmann, L., Karl, D. M., Iddaoud, G., and Gorsky, G.: The underwater vision profiler 5: an advanced instrument for high spatial resolution studies of particle size spectra and zooplankton, Limnol. Oceanogr.-Meth., 8, 462–473, doi:10.4319/lom.2010.8.462, 2010. 2210

OSD
10, 2207–2254, 2013

Pingree, R. D., Mardell, G. T., and Cartwright, D. E.: Slope turbulence, internal waves and phytoplankton growth at the celtic sea shelf-break [and discussion], Philos. T. R. Soc. A, 302, 663–682, doi:10.1098/rsta.1981.0191, 1981. 2229

Platt, T. and Denman, K.: Organization in Pelagic ecosystem, Helgoland. Wiss. Meer., 30, 575–581, 1977. 2215, 2229

Poulet, S. A., Laabir, M., and Chaudron, Y.: Characteristic features of zooplankton in the Bay of Biscay, Sci. Mar., 60, 79–95, 1996. 2210, 2211, 2212, 2228

Quintana, X. D., Brucet, S., Boix, D., Lopez-Flores, R., Gascon, S., Badosa, A., Sala, J., Moreno-Amich, R., and Egozcue, J. J.: A non-parametric method for the measurement of size diversity, with emphasis on data standardisation, Limnol. Oceanogr.-Meth., 6, 75–86, doi:10.4319/lom.2008.6.75, 2008. 2216

Rosipal, R., Kr, N., and Krämer, N.: Overview and recent advances in partial least squares, in: Subspace, Latent Structure and Feature Selection SE-2, edited by: Saunders, C., Grobelnik, M., Gunn, S., and Shawe-Taylor, J., vol. 3940 of Lecture Notes in Computer Science, Springer Berlin Heidelberg, 34–51, doi:10.1007/11752790_2, 2006. 2217

Schultes, S. and Lopes, R. M.: Laser optical plankton counter and zooscan intercomparison in tropical and subtropical marine ecosystems, Limnol. Oceanogr.-Meth., 7, 771–784, doi:10.4319/lom.2009.7.771, 2009. 2211, 2225, 2227

Sheldon, R. W., Sutcliffe, W. H., and Prakash, A.: The size distribution of particles in the ocean, Limnol. Oceanogr., 17, 327–340, doi:10.4319/lo.1972.17.3.0327, 1972. 2209

Sourisseau, M. and Carlotti, F.: Spatial distribution of zooplankton size spectra on the French continental shelf of the Bay of Biscay during spring 2000 and 2001, J. Geophys. Res., 111, 12–12, doi:10.1029/2005JC003063, 2006. 2211, 2225, 2226, 2229

Stemmann, L. and Boss, E.: Plankton and particle size and packaging: from determining optical properties to driving the biological pump, Annual Review of Marine Science, 4, 263–290, doi:10.1146/annurev-marine-120710-100853, 2012. 2209, 2212

Stemmann, L., Eloire, D., Sciandra, A., Jackson, G. A., Guidi, L., Picheral, M., and Gorsky, G.: Volume distribution for particles between 3.5 to 2000 µm in the upper 200 m region of the South Pacific Gyre, Biogeosciences, 5, 299–310, doi:10.5194/bg-5-299-2008, 2008. 2231

Suthers, L. M., Taggart, C. T., Rissik, D., Baird, M. E., and Suthers, I.: Day and night ichthyoplankton assemblages and zooplankton biomass size spectrum in a deep ocean island wake, Mar. Ecol.-Prog. Ser., 322, 225–238, doi:10.3354/meps322225, 2006. 2230

OSD
10, 2207–2254, 2013

Taylor, K. E.: Summarizing multiple aspects of model performance in a single diagram, J. Geophys. Res., 106, 7183, doi:10.1029/2000JD900719, 2001. 2222, 2247
Valdés, L., López-Urrutia, A., Cabal, J., Alvarez-Ossorio, M., Bode, A., Miranda, A., Cabanas, M., Huskin, I., Anadón, R., Alvarez-Marqués, F., Llope, M., and Rodríguez, N.: A decade of sampling in the Bay of Biscay: what are the zooplankton time series telling us?, Prog. Oceanogr., 74, 98–114, doi:10.1016/j.pocean.2007.04.016, 2007. 2211
Vandromme, P., Stemmann, L., Garcìa-Comas, C., Berline, L., Sun, X., Gorsky, G., Garcia-Comas, C., Colbert, S., Picheral, M., Gasparini, S., Guarini, J.-M., and Prejger, F.: Assessing biases in computing size spectra of automatically classified zooplankton from imaging systems: a case study with the ZooScan integrated system, Methods in Oceanography, 1–2, 3–21, doi:10.1016/j.mio.2012.06.001, 2012. 2210, 2211, 2214
Varela, M.: Phytoplankton ecology in the Bay of Biscay, Sci. Mar., 60, 45–53, 1996. 2213
Vidondo, B., Prairie, Y. T., Blanco, J. M., and Duarte, C. M.: Some aspects of the analysis of size spectra in aquatic ecology, Limnol. Oceanogr., 42, 184–192, doi:10.4319/lo.1997.42.1.0184, 1997. 2216
Ward, B. a., Dutkiewicz, S., Jahn, O., and Follows, M. J.: A size-structured food-web model for the global ocean, Limnol. Oceanogr., 57, 1877–1891, doi:10.4319/lo.2012.57.6.1877, 2012. 2210
Woodd-Walker, R. S., Gallienne, C. P., and Robins, D. B.: A test model for optical plankton counter (OPC) coincidence and a comparison of OPC-derived and conventional measures of plankton abundance, J. Plankton Res., 22, 473–483, doi:10.1093/plankt/22.3.473, 2000. 2213
Zhou, M., Carlotti, F., and Zhu, Y.: A size-spectrum zooplankton closure model for ecosystem modelling, J. Plankton Res., 32, 1147–1165, doi:10.1093/plankt/fbq054, 2010. 2218

OSD
10, 2207–2254, 2013

Table 1. Number of stations with LOPC and/or WP2/Zs data per cruises. There is a total of 816 LOPC profiles and 89 WP2 net samples analyzed with the ZooScan. The table shows also the starting and ending dates of the cruises.

Cruise	First station	Last station	#LOPC	#WP2/Zs
Pelacus 2005	5 Apr	29 Apr	100	0
Pelgas 2005	5 May	30 May	52	0
Pelacus 2006	3 Apr	18 Apr	43	0
Pelacus 2007	11 Apr	21 Apr	55	14
Pelgas 2007	27 Apr	18 May	55	0
Pelacus 2009	2 Apr	20 Apr	77	0
Pelgas 2009	26 Apr	2 Jun	105	24
Pelgas 2010	26 Apr	2 Jun	117	23
Pelgas 2011	29 Apr	3 Jun	127	29
Pelgas 2012	27 Apr	24 May	85	0
		$\sum =$	816	89

OSD
10, 2207–2254, 2013

Table 2. Results of the stepwise Redundancy Analysis (RDA) and simple RDA performed on residuals from NBSSs of [LOPC-WP2/Zs]. ~~See text for details on the procedure.~~ Par. F = partial F-statistic; Cum. Exp. = cumulative fraction of variance explained; Tot. Expl. = fraction of the total variance explained; Tot. F = total F-statistic; p = p values for significance of the F-statistic; Sat. = Satellite; T° = temperature; surf. = surface; stratif. = stratification; Sal. = salinity; fluo = fluorescence; MLD = mixed layer depth; SPM = suspended particulate matter; Int. = Integrated (from surface to a max of 100 m depth); d-7/14 = Satellite data 7 and 14 days before the sampling date. The last column represent the direction of the correlation with respectively the slope and the intercept of the residuals (i.e., the non-living matter).

	Stepwise RDA			Simple RDA			
Variables	Cum. Exp.	Par. F	p	Tot. expl.	Tot. F	p	
LOPC biomass	0.40	55.02	0.01	0.4	55.02	0.01	+ +
Sat. chla	0.52	20.78	0.01	0.01	0.82	0.01	+ –
Bathymetry	0.56	7.68	0.01	0.02	1.29	0.01	– –
LOPC slope	0.59	6.28	0.01	0.25	28.41	0.01	+ –
Density bottom	0.61	3.55	0.22	0.06	5.77	0.01	– –
T° bottom	0.62	2.90	0.12	0.01	0.63	0.52	– +
Salinity bottom	0.66	7.89	0.01	0.03	2.85	0.01	– –
Sat chla d-7	0.68	5.61	0.01	0.05	4.47	0.15	+ +
Julian day	0.69	2.24	0.23	0.12	11.31	0.01	+ –
Latitude	0.70	1.94	0.22	0.09	8.64	0.01	+ –
Sat. chla d-14	0.70	1.09	0.11	0.01	1.09	0.24	+ +
Sat. SPM d-7	0.70	0.84	0.47	0.01	0.43	0.48	+ +
Strat. mean	0.71	1.32	0.21	0.02	1.96	0.35	+ +
Sat. SPM d-14	0.71	0.60	0.30	0.00	0.33	0.64	+ +
Depth of fluo. max	0.71	0.30	0.76	0.01	1.11	0.29	– –
MLD	0.71	0.15	0.6	0.03	2.61	0.01	– –
Coast dist.	0.71	0.11	0.91	0.07	6.29	0.01	– –
Fluo. max	0.71	0.07	0.81	0.00	0.32	0.75	+ +
Sat. SPM	0.72	0.08	0.91	0.02	1.42	0.34	+ +
T° surf.	0.72	0.04	1.00	0.02	2.04	0.30	– –
Strat. max	0.72	0.05	0.91	0.07	5.88	0.01	+ +
Salinity surf.	0.72	0.04	0.91	0.06	5.67	0.01	– –
Density surf.	0.73	3.33	0.10	0.04	3.26	0.14	+ –
Fluo. int.	0.73	0.00	1.00	0.00	0.01	1.00	– +

OSD
10, 2207–2254, 2013

Table 3. Stepwise Redundancy Analysis (RDA) performed with environmental data (as in Table 2) and with fractionated chlorophyll *a* (three fractions) from Pelgas 2009, 2010 and 2011 (total of 68 stations located in the French Shelf of the Bay of Biscay). Only the cumulative explained variance is displayed (Cum. Exp.) for the 5 first explanatory variables, the first chlorophyll *a* fraction (plus the variable just before) and the last one. On the same ~~68 stations~~, environmental data only explained 0.74 of the total variance.

Variables	Cum. Exp.
LOPC biomass	0.41
chl 3	0.51
Bathymetry	0.56
chl 2	0.59
Fluo. int.	0.60
...	
LOPC slope	0.72
chl 1	0.73
...	
Depth of fluo. max	0.80

OSD
10, 2207–2254, 2013

Table 4. Stepwise Redundancy Analysis (RDA) performed with zooplankton group abundances from Pelgas 2009, 2010 and 2011 as explanatory variables (total of 75 stations located in the French Shelf of the Bay of Biscay). Here only the cumulative explained variance is displayed (Cum. Exp.) for the 5 first zooplankton groups and the last one. On the same ~~75~~ stations, environmental data only (as in Table 2) explained 0.71 of the total variance.

Variables	Cum. Exp.
Acartia sp.	0.49
cladocerans	0.66
Calanus sp.	0.76
small calanoids	0.82
larvaceans	0.87
...	
Limacina sp.	0.92

OSD
10, 2207–2254, 2013

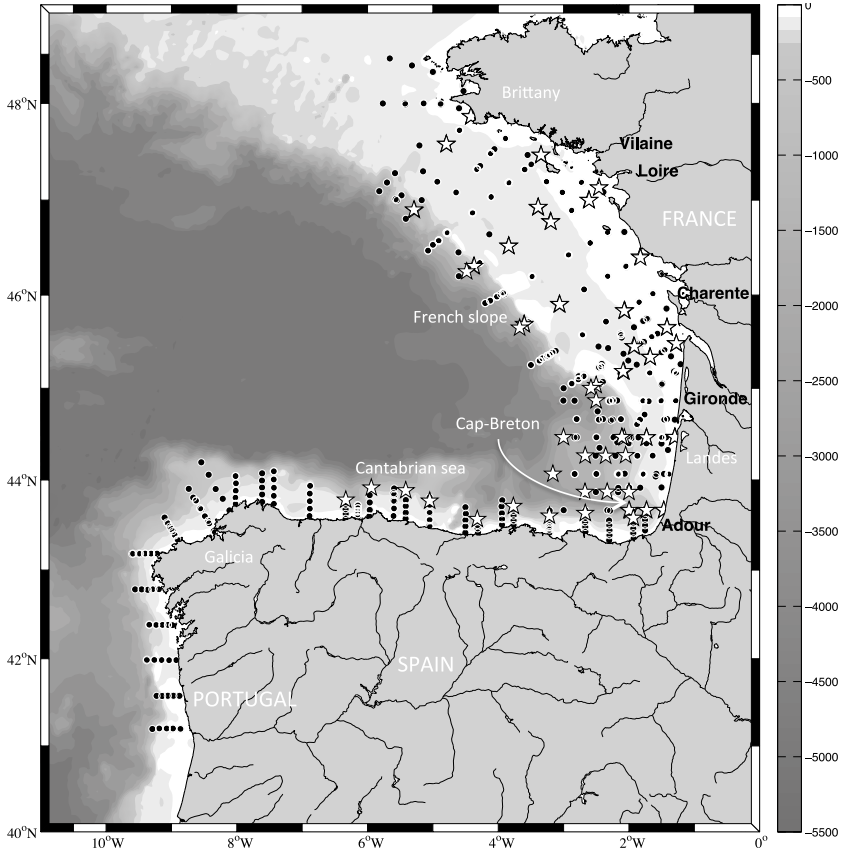

Fig. 1. Bathymetry of the Bay of Biscay and location of stations (black circle for LOPC only and white star for LOPC and WP2 net). Location and name of main rivers are indicated in black whereas geographical name are indicated in white.

OSD
10, 2207–2254, 2013

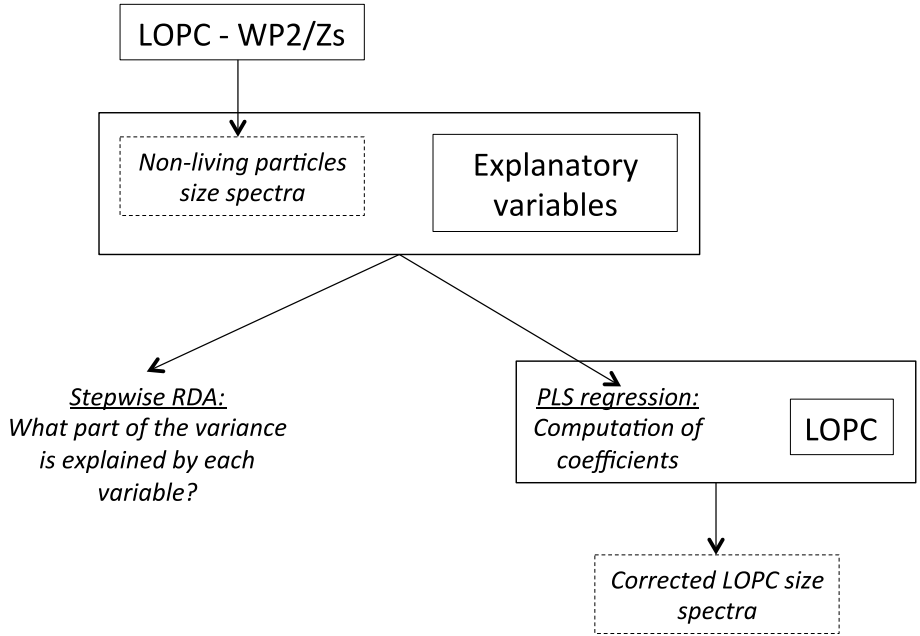

Fig. 2. Diagram showing the different analyses performed on the LOPC dataset.

OSD
10, 2207–2254, 2013

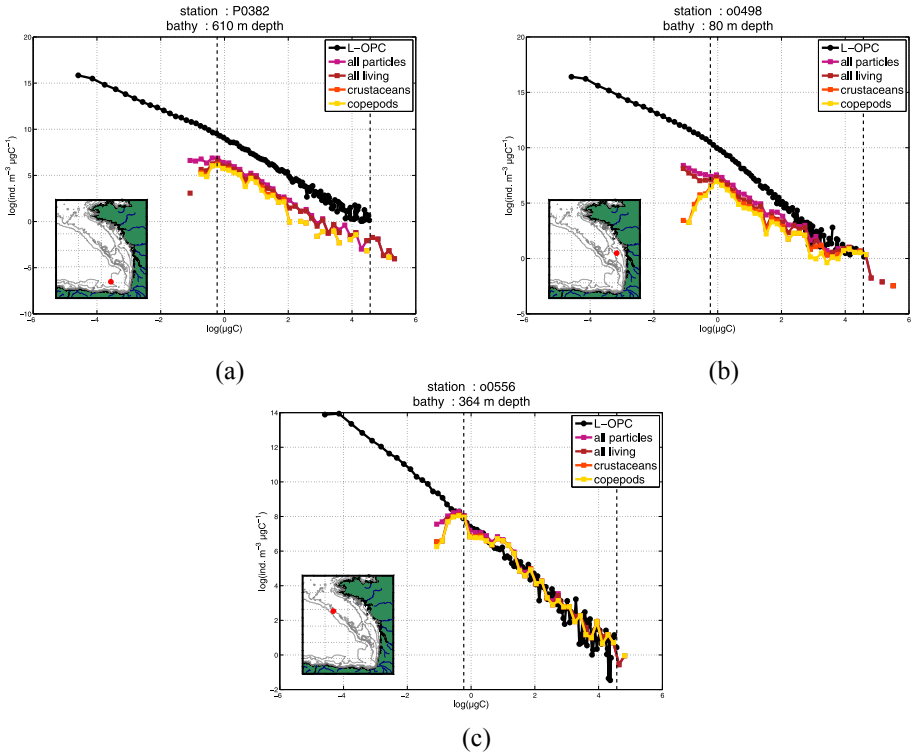

Fig. 3. Examples of simultaneous Normalized Biomass Size Spectra (NBSS) measured by the LOPC and by the WP2/Zs~~. For the WP2/Zs~~ the NBSS of all objects, all zooplankton, all crustaceans and copepods only ~~are shown~~. The two vertical dash lines indicate the limits of comparable size classes of the LOPC and the WP2/Zs. ~~Location of station is shown ss insets of each graph. **(a)** shows an example where the LOPC overestimates the WP2/Zs for all size classes, **(b)** where the overestimation is only for smaller size classes and **(c)** where there is no overestimation.~~

OSD
10, 2207–2254, 2013

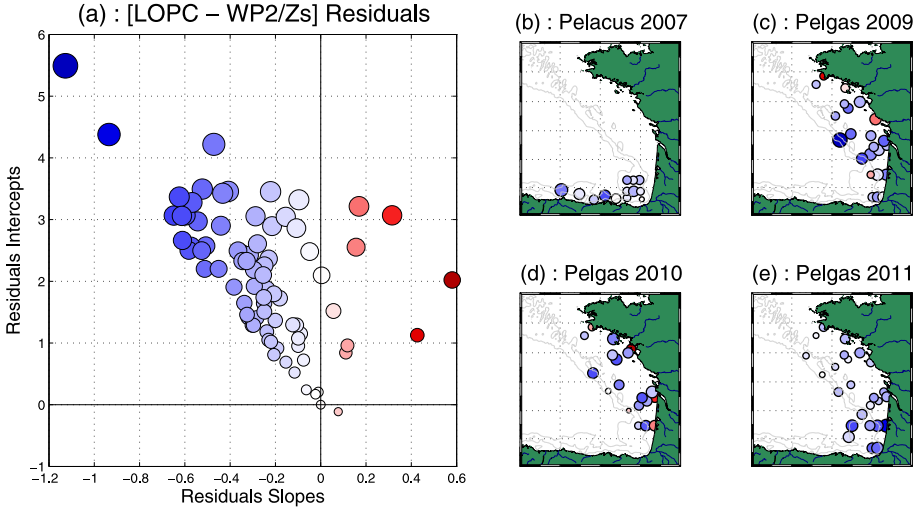

Fig. 4. Size structure characteristics of residuals between NBSS estimated by the LOPC and by the WP2/Zs procedure. ~~**(a)** shows the relation between the slope and the intercept of residuals. the~~ colormap indicates the value of the slope of the residuals (blue for negative slope, red for positive ones and white for null slopes). The size of points indicates the value of the intercept of residuals (the bigger the points, the larger the intercepts). **(b–e)** show the spatial distribution of residuals for the four cruises in which ~~we have~~ data for both LOPC and WP2/Zs (Pelacus 2007 ~~**(b)**~~, Pelgas 2009 ~~**(c)**~~, Pelgas 2010 ~~**(d)**~~ and **(e)** Pelgas 2011). ~~The color are the same as in **(a)**~~ but ~~for clarity~~ size of points ~~have been~~ divided by three.

OSD
10, 2207–2254, 2013

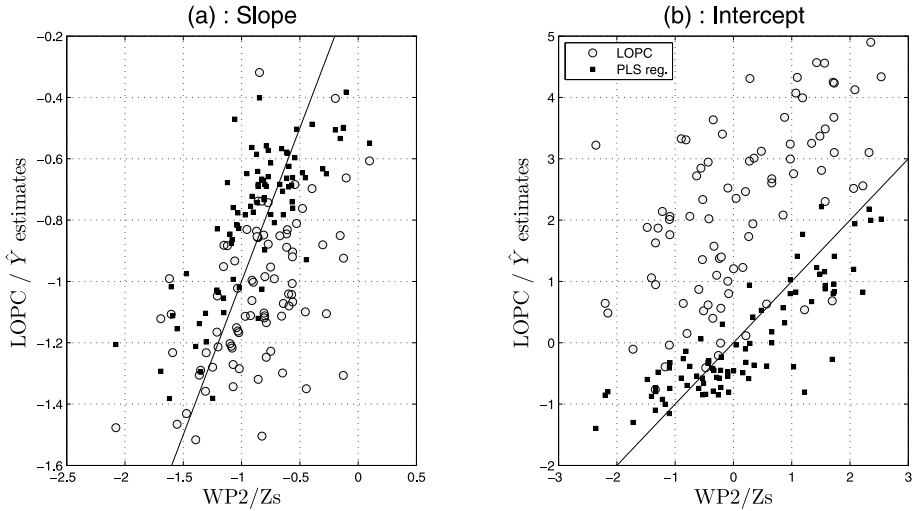

Fig. 5. Scatter graph of the relations of NBSS slopes **(a)** and intercepts **(b)** estimated by the WP2/Zs vs. the raw LOPC (grey points), and after the PLS (Partial Least Square) regression was performed on the LOPC ($\hat{Y}$, black plain square). The $x = y$ line is added to each plot.

OSD
10, 2207–2254, 2013

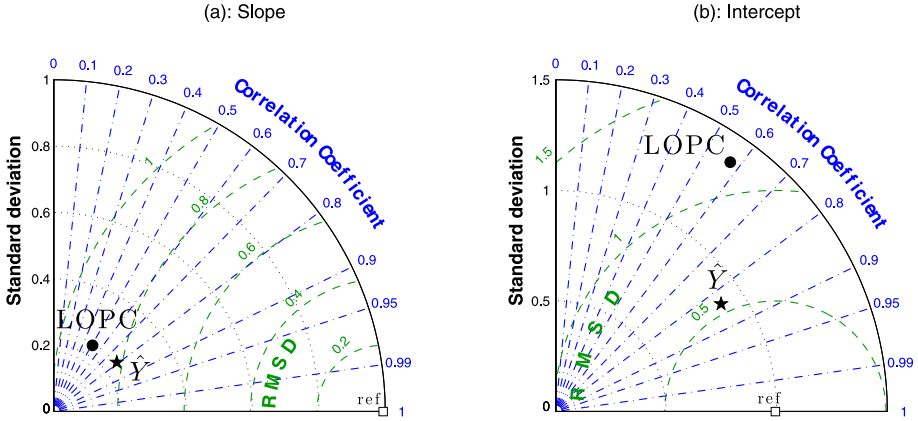

Fig. 6. Taylor diagram (Taylor, 2001) of the correlation (R), the centered root mean square difference (RMSD) and standard deviation (STD) between NBSS parameters (**a**: slope and **b**: intercept) estimated by the WP2/Zs and estimated by the LOPC (black plain circles) and after the PLS (Partial Least Square) regression performed on the LOPC ($\hat{Y}$, black plain stars). The white square indicates the maximum (R = 1, RMSD = 0 and STD = 1).

OSD
10, 2207–2254, 2013

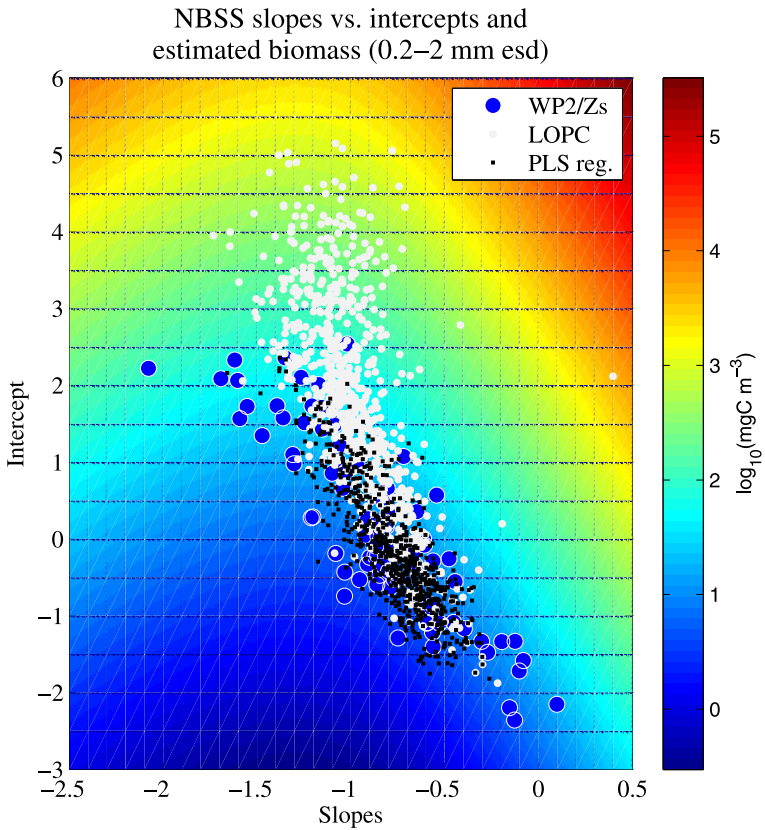

Fig. 7. Scatter graph of the relations between slopes and intercepts computed from NBSS estimated by the WP2/Zs (blue circles), the LOPC (grey circles) and by the PLS (Partial Least Square) regression (black square). The colormap corresponds to the biomass computed as the integration of the log-linear NBSS in the range 0.2–2 mm ESD.

OSD
10, 2207–2254, 2013

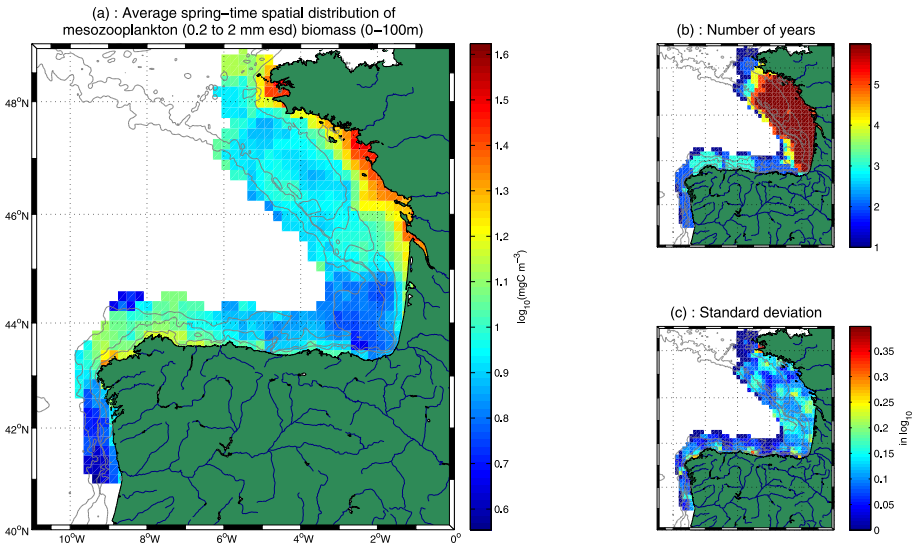

Fig. 8. Spatial distribution of mesozooplankton (from 0.2 to 2 mm ESD) biomass concentration (in $\log_{10}$ mg C m^{-3}) from the surface to a maximum of 100 m depth and calculated as the integral of the NBSS estimated by the PLS (Partial Least Square) regression. A regular grid was generated each year and nodes were interpolated from available data within a radius of 30 km and weighted by the square of their distance. **(a)** shows the average distribution, **(b)** the total number of year used to calculate each points and **(c)** shows the standard deviation.

OSD
10, 2207–2254, 2013

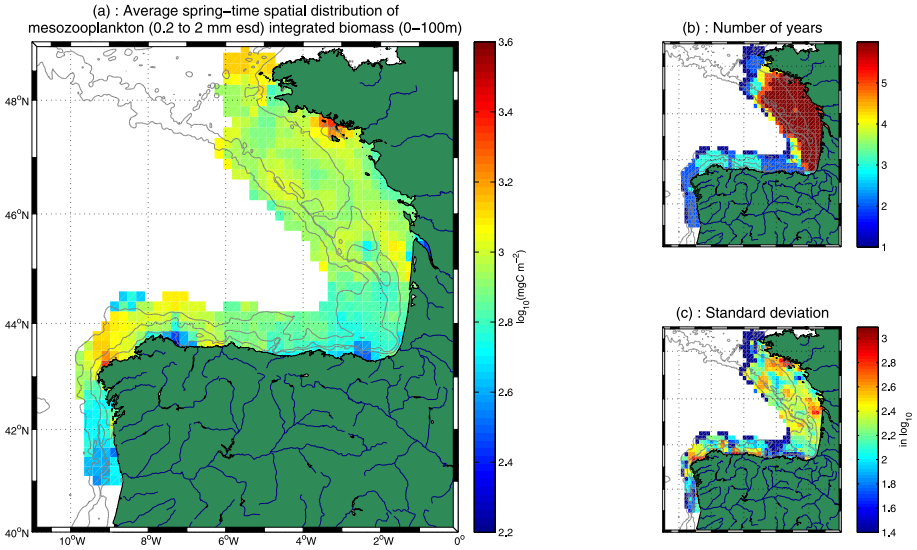

Fig. 9. Spatial distribution of mesozooplankton (from 0.2 to 2 mm ESD) integrated biomass (in $\log_{10}$ mg C m^{-2}) ~~from the surface to a maximum of 100 m depth and calculated as the integral of the NBSS estimated by the PLS (Partial Least Square) regression. A regular grid was generated each year and nodes were interpolated from available data within a radius of 30 km and weighted by the square of their distance~~. **(a)** shows the average distribution, **(b)** the total number of year used to calculate each points and **(c)** shows the standard deviation.

OSD
10, 2207–2254, 2013

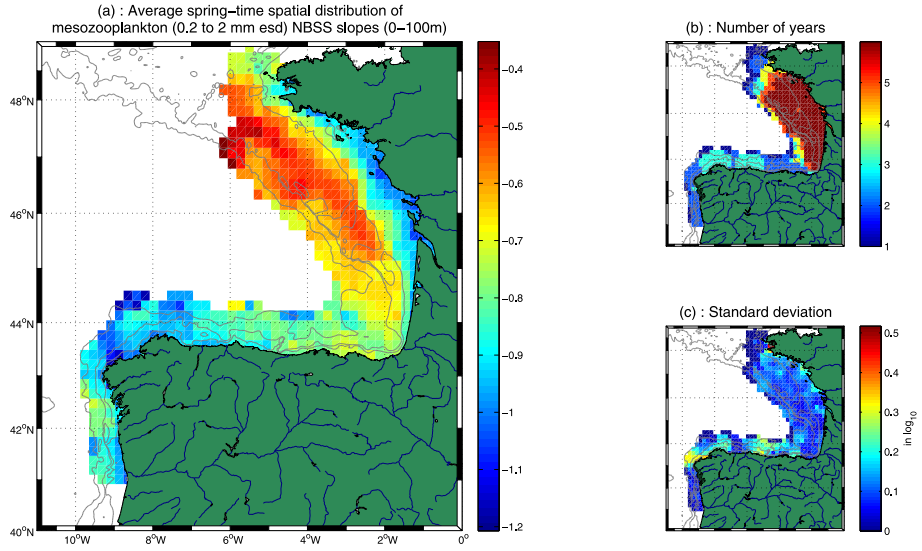

Fig. 10. Spatial distribution of NBSS slopes estimated by the PLS (Partial Least Square) regression. ~~A regular grid was generated each year and nodes were interpolated from available data within a radius of 30 km and ponderated by the square of their distance.~~ **(a)** shows the average distribution, **(b)** the total number of year used to calculate each points and **(c)** shows the standard deviation.

OSD
10, 2207–2254, 2013

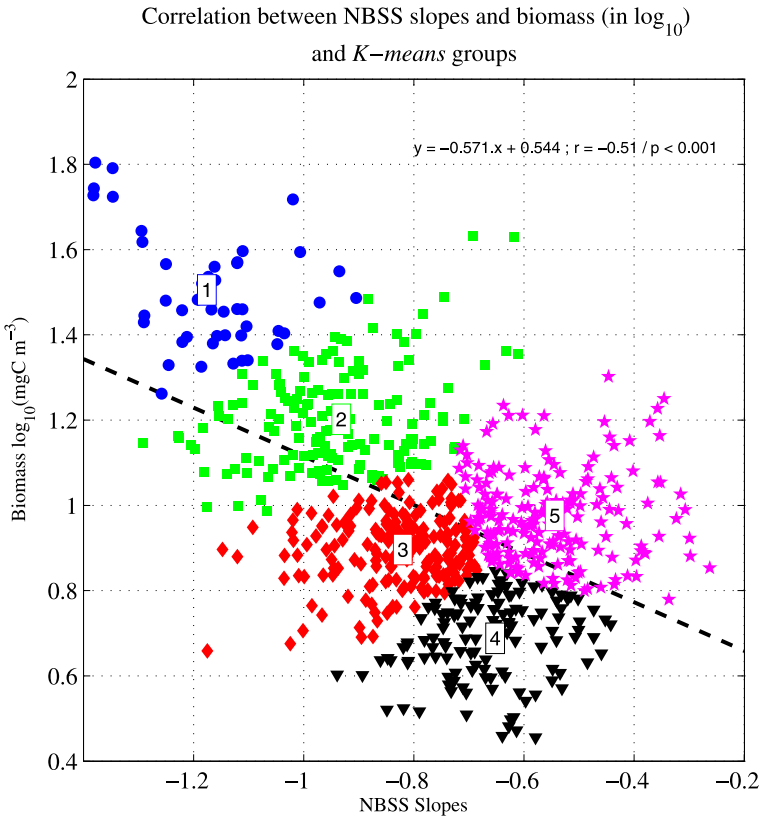

Fig. 11. Correlation between slopes and the biomass computed as the integration of the log-linear NBSS in the range 0.2–2 mm ESD. The correlation (Pearson) is significant with a $r = -0.51$. Result of a 5 groups K means clustering based on estimated slope and biomass is shown with differents colors and shapes. Group 1: blue circles, group 2: green squares, group 3: red losanges, group 4: black triangles and group 5: pink stars.

OSD
10, 2207–2254, 2013

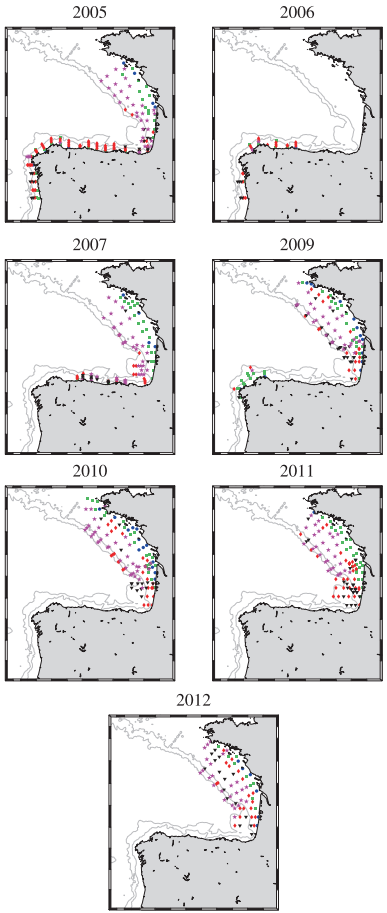

Fig. 12. Spatial and interannual distribution of *K* means groups as established in Fig. 11 for the seven years. Groups are represented by the same colors and shapes as in Fig. 11.

OSD
10, 2207–2254, 2013

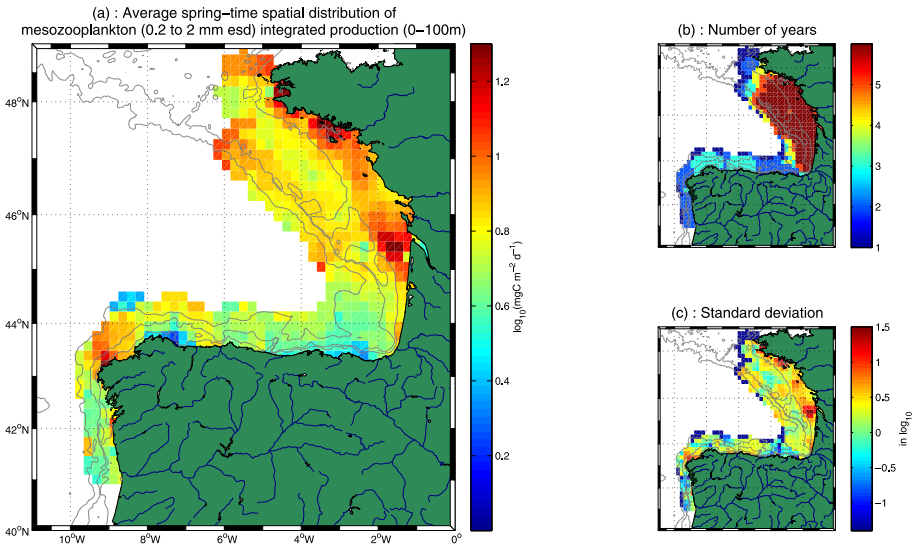

Fig. 13. Spatial distribution of mesozooplankton (from 0.2 to 2 mm ESD) productivity (in $\log_{10}$ mg C m^{-2} d^{-1}) calculated from the NBSS estimated by the PLS (Partial Least Square) regression ~~(Sect. 2.4)~~. ~~A regular grid was generated each year and nodes were interpolated from available data within a radius of 30 km and ponderated by the square of their distance.~~ **(a)** shows the average distribution, **(b)** the total number of year used to calculate each points and **(c)** shows the standard deviation.

OSD
10, 2207–2254, 2013